MIXING ENHANCEMENT IN LAMINAR FLOW USING INCLINED INVERTED *L*-SHAPED VORTEX GENERATORS

by

Omolayo M. IKUMAPAYI[a], Mohammed DOUHA[b], Samia LARGUECH[c], Noureddine KAID[d], Younes MENNI[d,e], Mustafa BAYRAM[f*], Abiodun BAYODE[a], Tin Tin TING[g,h], Erdinc VURAL[i], and Salih OZER[j]

[a] Department of Mechanical Engineering, Northwest University, Potchefstroom, South Africa
[b] Higher Normal School of Bechar, Bechar, Algeria
[c] Department of Electrical Engineering, College of Engineering, Princess Nourah bint Abdulrahman University, Riyadh, Saudi Arabia
[d] Department of Mechanical Engineering, Institute of Technology, University Center Salhi Ahmed Naama (Ctr. Univ. Naama), Naama, Algeria
[e] College of Technical Engineering, National University of Science and Technology, Dhi Qar, Iraq
[f] Department of Computer Engineering, Biruni University, Istanbul, Turkey
[g] Faculty of Data Science and Information Technology, INTI International University, Nilai, Malaysia
[h] School of Information Technology, UNITAR International University, Selangor, Malaysia
[i] Germencik Yamanturk Vocational School, Aydin Adnan Menderes University, Aydin, Turkiye
[j] Mus Alparslan University, Mechanical Engineering, Mus, Turkiye

Original scientific paper
https://doi.org/10.2298/TSCI2504211I

This study presents a numerical investigation of the mixing performance and hydraulic behavior of a static mixer equipped with staggered inverted L-shaped vortex generators mounted on both the upper and lower walls of a rectangular channel, operating under laminar flow conditions. The working fluid is Newtonian with properties similar to water, and mixing is initiated by the introduction of two inlet streams with a step-change in concentration. The effects of Reynolds number (Re = 20-600) and vortex generators inclination angles (30°, 45°, 60°) on mixing efficiency and pressure drop are systematically evaluated. Results show that higher vortex generators inclination angles significantly enhance mixing at low to moderate Reynolds number due to stronger secondary flows and increased interfacial deformation. However, this improvement is accompanied by a notable rise in pressure drop. At higher Reynods number, the 30° configuration achieves a mixing index of 0.9468 with a pressure drop 78% lower than the 60° case, demonstrating a more favorable balance between mixing and energy consumption. The optimal configuration is found at a vortex generators inclination of 30° and Re = 600, offering efficient mixing with reduced hydraulic resistance.

Key words: *static mixer, vortex generators, laminar flow, mixing index, pressure drop*

Introduction

Static mixers are vital components in modern process industries due to their ability to enhance mixing, heat transfer, and mass transport without moving parts. Their compact structure, low maintenance requirements, and energy efficiency make them ideal for applications

* Corresponding author, e-mail: mustafabayram@biruni.edu.tr

across chemical processing, polymerization, heat exchange, and micro-fluidics. As mixing requirements become more complex, recent research has focused on optimizing mixer geometry and internal structures to improve performance under laminar, transitional, and turbulent flow regimes. One of the prominent strategies involves geometric enhancement through corrugated walls and internal baffles. Bennour *et al*. [1, 2], Kaid *et al*. [3], and Menni *et al*. [4] demonstrated that incorporating corrugations and vortex-generating baffles significantly enhances mixing quality and heat transfer, especially for shear-thinning fluids. These structures induce secondary flow patterns and promote chaotic advection, crucial for homogeneous mixing in laminar flow conditions. Another focus has been on advanced blade-type and twisted insert configurations. Meng *et al*. [5-7] and Yu *et al*. [8] explored multitwisted leaves, Kenics blades, and tape-based inserts, revealing marked improvements in mixing efficiency and thermal uniformity. In particular, Yu *et al*. [9] provided a detailed numerical investigation into blade-type static mixers, analyzing their performance in terms of mixing index and thermal distribution. In efforts to reduce pressure drop while maintaining effective mixing, researchers like Liao and Jing [10] and Bennour *et al*. [1] investigated flexible vortex generators and low pressure loss insert designs. Kaid *et al*. [3] confirmed the effectiveness of passive structures in achieving high mixing performance at minimal energy costs. The combination of experimental validation and numerical modelling has greatly accelerated mixer development. Fan *et al*. [11], Kundra *et al*. [12], and Albertazzi *et al*. [13] demonstrated the industrial relevance of novel mixers through pilot-scale and continuous-flow studies. The CFD simulations by Coroneo *et al*. [14], Cheng *et al.* [15], and Chakleh and Azizi [16] enabled predictive analysis of flow fields and mixing profiles, guiding optimized design under various flow conditions.

Microscale static mixing has also attracted increasing attention. Bennour *et al*. [17], Faradonbeh *et al*. [18], and Fallah *et al*. [19] explored designs incorporating chambers, deformable beams, and acoustic effects to enhance mixing in micro-fluidic systems, particularly for biomedical and non-Newtonian fluid applications. Basu and Dirbude [20] further examined scalar transport behavior in miniaturized *T*-shaped configurations.

Energy consumption and flow resistance remain key constraints in mixer design. Studies by Wang *et al*. [21], Stec and Synowiec [22], and Rauline *et al*. [23] investigated pressure drop behavior across various geometries, offering insights into the trade-offs between mixing performance and hydraulic efficiency. Meng *et al.* [24] examined the use of nanofluids in multi-blade static mixers to enhance thermal performance. In addition, Yu *et al*. [25] provided a comprehensive review of gas-liquid two-phase flow in static mixers, summarizing current advances, flow regimes, and performance evaluation criteria, and offering valuable guidance for future research and design development in multi-phase mixing applications.

Innovative concepts such as perforated mixers [21], side-injection reactors [13], and concentric double-helix blades [4] continue to evolve, supported by performance comparisons with commercial designs [16] and multi-objective optimization frameworks [8]. These advancements have yielded mixers with significantly improved thermal and mixing indices, tailored for diverse operational needs.

The present study is motivated by the need to develop high efficiency static mixers capable of achieving enhanced mixing performance while minimizing energy losses, particularly in compact flow systems. To this end, we investigate a novel 3-D mixer configuration featuring a rectangular channel equipped with inverted *L*-shaped vortex generators (VG). This geometry is designed to induce secondary flows and promote chaotic advection, thereby improving mixing quality. The primary aim is to evaluate the mixing behavior through detailed analysis of molar concentration contours, contact probability distributions, mixing index values, and

pressure drop characteristics across a range of flow rates. Furthermore, the study systematically explores the influence of the inclination angle of the VG in combination with varying Reynolds numbers to identify the optimal design configuration. By examining the coupled effects of flow dynamics and geometric orientation, this research seeks to propose a geometrically optimized static mixer that offers superior mixing efficiency with minimal hydraulic penalty.

Physical configuration and numerical approach

This study investigates a 3-D static mixer consisting of a rectangular channel equipped with inverted *L*-shaped VG arranged in a staggered configuration on both the upper and lower walls. The VG are inclined at angles of 30°, 45°, and 60° relative to the main flow direction and are uniformly spaced along the length of the channel. Additionally, flat barriers are positioned between the walls and located between the *L*-shaped baffles along the channel. These obstacles serve to induce secondary flows, enhancing fluid deformation and promoting transverse mixing. The top and bottom walls of the channel are treated as adiabatic, thereby preventing heat transfer across these surfaces. As shown in fig. 1, the geometric configuration includes regularly spaced inverted *L*-shaped VG, clearly illustrating the staggered arrangement along the channel walls.

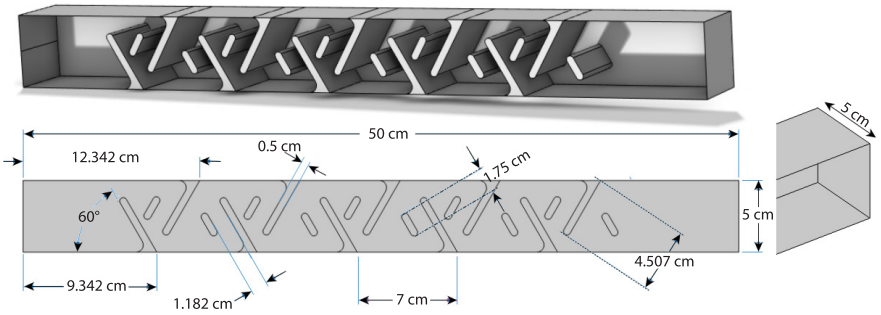

Figure 1. Flow domain with upper, lower, and central obstacles

Mixing is initiated by introducing two distinct streams at the inlet: pure water (with tracer concentration (c = 0 mol/m^3) enters through the lower half of the inlet cross-section, while dyed water (with tracer concentration c = 1 mol/m^3) enters through the upper half. This creates an initial step concentration profile that allows for clear observation of mixing evolution downstream.

The fluid is assumed to be Newtonian, with physical properties analogous to water: density ρ = 998 kg/m^3, and dynamic viscosity μ = 0.001 Pa·s. Flow conditions are steady, incompressible, and laminar, with Reynolds numbers ranging from 20-600. A uniform velocity profile is applied at the inlet, while the outlet is subjected to atmospheric pressure. No-slip boundary conditions are imposed on all solid surfaces, including the obstacles.

The flow and mixing are governed by the following equations.

Continuity equation:

$$\nabla\vec{u} = 0 \tag{1}$$

Momentum equation:

$$\rho\left(\vec{u}\nabla\right)\vec{u} = -\nabla p + \mu\nabla^2\vec{u} \tag{2}$$

Convection-diffusion equation:

$$\vec{u}\nabla c = \Gamma\nabla^2 c \tag{3}$$

where $\vec{u}$ is the velocity vector and Γ – the diffusion coefficient. To quantitatively evaluate mixing efficiency along the channel, a mixing index *MI* is used. This index measures the degree of concentration uniformity and is defined:

$$MI = 1 - \frac{\sqrt{\frac{1}{N}\sum_{i=1}^{N}(c_i - \bar{c})^2}}{\bar{c}} \tag{4}$$

where c_i is the local tracer concentration at the i^{th} cell, $\bar{c}$ – the mean tracer concentration across the cross-section, and N – the total number of cells in the sampling cross-section.

As shown in fig. 2, the computational domain is discretized using a hybrid mesh generated for the FEM, totaling 1485285 elements. This includes 1291773 tetrahedral elements for the main volume, 193512 prismatic elements strategically placed near-walls to improve boundary-layer resolution, and 107467 triangular along with 276 quadrilateral surface elements for accurate boundary representation. The mesh achieves an average quality of 0.6795, while the minimum quality reaches 0.01356, reflecting the geometric complexity of the mixer configuration.

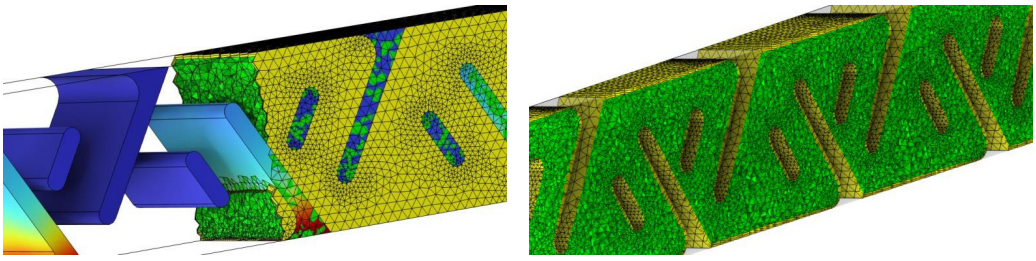

Figure 2. Computational mesh of the studied static mixer equipped with VG and barriers

To validate the numerical model, the computed friction factor for the present smooth channel is compared with the theoretical values from the Moody correlation for fully developed laminar flow, eq. (5), over the present range of studied Reynolds numbers (20-600) :

$$f = \frac{64}{\mathrm{Re}} \tag{5}$$

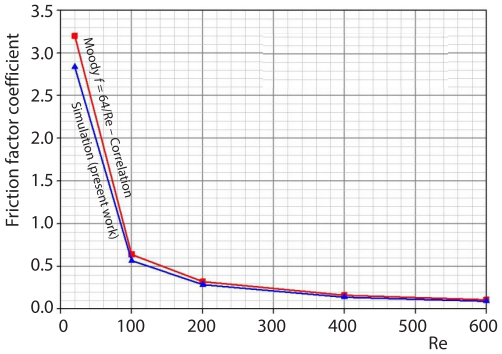

Figure 3. Friction factor comparison between numerical results and Moody correlation

As shown in fig. 3, the comparison demonstrates good agreement, confirming the accuracy and reliability of the numerical approach within the investigated flow regime.

Results and discussion

To evaluate the impact of VG inclination and flow conditions on mixing performance, molar concentration contours were examined at various Reynolds numbers for different VG configurations. Figure 4 presents the molar concentration distributions at Reynolds numbers of 20, 200, and 600 for three inclination angles (30°, 45°, and 60°) of inverted *L*-shaped VG installed within the mixing channel. In fig. 4(a), corresponding to Re = 20, the flow is dominated by viscous and diffusive effects, resulting

in limited mixing. The concentration field exhibits strong stratification, particularly for the 30° and 45° configurations, with only mild interfacial deformation observed. The 60° VG configuration shows a modest improvement due to stronger induced secondary flows, which promote slight stretching and folding of the interface between the dyed and undyed streams.

As seen in fig. 4(b), at Re = 200, convective transport becomes more dominant, and mixing performance improves significantly. The higher VG inclinations, especially at 60°, enhance the formation of complex 3-D flow structures, leading to greater interfacial renewal and more effective radial redistribution of the tracer. At Re = 600, illustrated in fig. 4(c), inertial effects prevail, and the flow becomes highly structured, with intense vortex activity and transverse flow components. The 60° configuration achieves near-complete homogenization of the tracer concentration at the outlet, while the 30° and 45° cases still show visible, though reduced, concentration gradients.

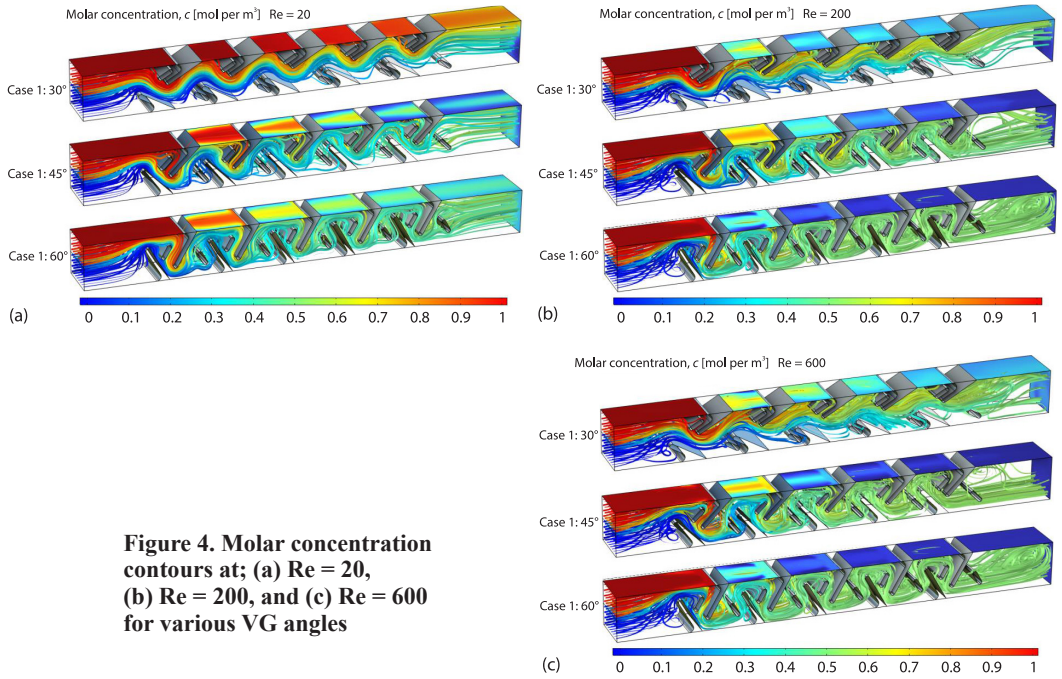

Figure 4. Molar concentration contours at; (a) Re = 20, (b) Re = 200, and (c) Re = 600 for various VG angles

The observed improvements in mixing with increasing Reynolds number and VG inclination angle highlight the strong influence of flow inertia and geometric configuration on mixing efficiency. The staggered arrangement of inverted *L*-shaped VG, coupled with central obstacles, contributes to enhanced fluid splitting, reorientation, and convective mixing throughout the channel.

Contact probability fields, ranging from 0 (unmixed) to 1 (fully mixed), demonstrate a strong dependence on both the Reynolds number and the inclination angle of the inverted *L*-shaped VG, as illustrated in fig. 5. Figure 5(a) shows the distribution of contact probability at Re = 20 for VG inclination angles of 30°, 45°, and 60°, where mixing remains limited due to the dominance of viscous and diffusive effects. At this low Reynold number, fluid deformation and interfacial renewal are weak, especially at 30°, resulting in poor mixing across the channel. In contrast, fig. 5(b) presents the case for Re = 200, where convective transport becomes more influential. Here, increased VG inclination enhances secondary flow intensity and fluid

interpenetration, with the 60° configuration exhibiting more advanced development of high contact probability regions. The most substantial improvements are observed in fig. 5(c), corresponding to Re = 600, where inertial effects dominate. At this higher Reynolds number, the VG induce strong cross-stream motion and complex 3-D vortices that significantly increase interfacial area and accelerate homogenization. The 60° inclination again outperforms the lower angles, leading to nearly complete mixing over a short axial distance. Overall, the contour plots in fig. 5 highlight the synergistic role of VG geometry and flow regime, with a 60° inclination at higher Reynolds numbers (≥200) yielding the most effective mixing through enhanced convective transport and intensified secondary flow structures.

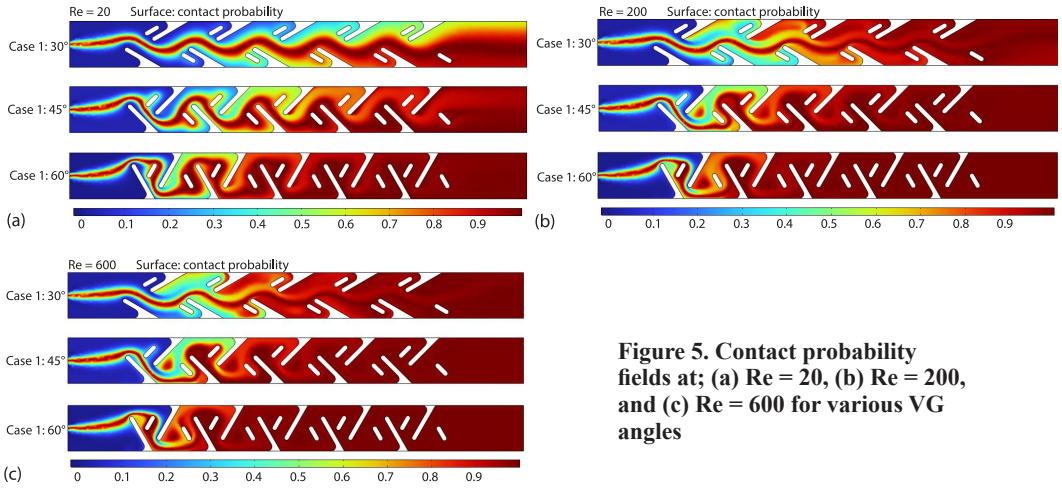

Figure 5. Contact probability fields at; (a) Re = 20, (b) Re = 200, and (c) Re = 600 for various VG angles

The pressure drop across the static mixer increases markedly with rising Reynolds number and varies significantly with the inclination angle of the VG, as illustrated in fig. 6. At Re = 600, the 60° configuration generates a pressure drop of 33.3160 Pa, compared to just 7.0194 Pa for the 30° set-up, an increase of approximately 375%, meaning the 60° design induces more than 4.7 times the resistance. At lower Reynolds numbers, this contrast is still evident; for instance, at Re = 100, the 60° angle causes a pressure drop of 1.1444 Pa, which is 679% higher than the 0.1468 Pa observed for 30°. Even at Re = 20, the pressure drop at 60° (0.0888 Pa) is about 599% greater than at 30° (0.0127 Pa). These trends, clearly depicted in fig. 6, demonstrate how the steeper VG angle consistently imposes a substantial energy penalty across all flow conditions, with pressure drops ranging from 6-7 times higher than those of the shallower 30° design. While increased VG inclination improves fluid mixing, it also leads to significantly greater flow resistance and energy consumption.

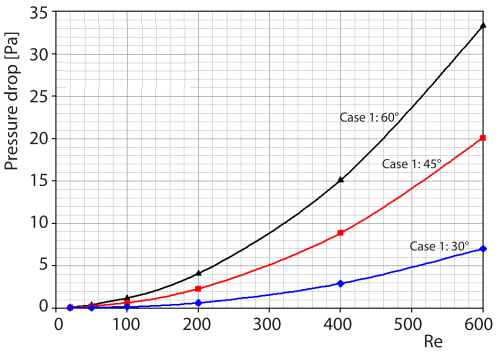

Figure 6. Pressure drop response to flow rate and VG inclination angle variations

The variation of the mixing index with Reynolds number and VG inclination angle reveals clear trends in mixing efficiency throughout the operational range, as supported by fig. 7. At a fixed inclination of 60°, the mixing index improves rapidly from 0.9121 at Re = 20 to a peak of 0.9891 at Re = 100, indicating enhanced blending due to stronger convective effects. Howev-

er, beyond Re = 100, the mixing index gradually declines to 0.9399 at Re = 600, suggesting a slight deterioration in mixing uniformity due to excessive flow inertia and possible flow channeling. A similar pattern is observed for the 45° configuration, where the mixing index rises from 0.8294 at Re = 20 to 0.9542 at Re = 200, then slightly drops to 0.9257 at Re = 600. In contrast, the 30° inclination shows a continuous upward trend, with the index increasing from 0.6475 at Re = 20-0.9468 at Re = 600, surpassing both 60° and 45° at the highest Reynolds number. These observations indicate that while steep VG angles (*e.g.*, 60°) are more effective at lower Reynolds numbers due to stronger secondary flows and fluid stretching, shallower configurations (*e.g.*, 30°) become more favorable at high Reynolds number by offering sufficient mixing with less energy loss and reduced vortex dissipation. This change in performance shows that the way mixing happens depends on the flow speed. At low Reynolds numbers, mixing is mainly due to diffusion, while at high Reynolds numbers, it is driven by fluid motion and inertia. This means that choosing the right VG angle depends on the flow conditions to get the best mixing results.

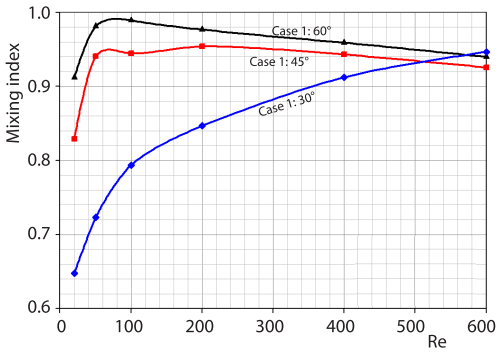

Figure 7. Mixing index trends for different flow rates and VG inclination angles

Conclusions

This study examined the mixing and hydraulic performance of a static mixer equipped with staggered inverted *L*-shaped VG, focusing on the effects of VG inclination angle and Reynolds number. Numerical results showed that increasing both VG angle and Reynolds number generally enhances mixing due to stronger secondary flows and convective transport. Specifically, the 60° inclination produced the most effective mixing at low-to-moderate Reynolds numbers, achieving a peak mixing index of 0.9891 at Re = 100. However, this configuration also caused significantly higher pressure drops, up to 33.3160 Pa at Re = 600, which is approximately 375% higher than that of the 30° design at the same Reynolds number.

In contrast, the 30° VG configuration demonstrated a remarkable balance at higher Reynolds numbers. At Re = 600, it achieved the highest mixing index of 0.9468 while maintaining a relatively low pressure drop of 7.0194 Pa, making it the most energy-efficient option. The 45° case offered intermediate performance but did not outperform either extreme across the evaluated range.

Considering both mixing effectiveness and energy consumption, the optimal configuration is the 30° VG inclination at Re = 600. This set-up delivers excellent mixing comparable to steeper VG angles, while significantly reducing the pressure drop, making it ideal for high through put or energy sensitive applications.

Acknowledgment

Princess Nourah bint Abdulrahman University Researchers Supporting Project number (PNURSP2025R826), Princess Nourah bint Abdulrahman University, Riyadh, Saudi Arabia.

References

[1] Bennour, E., *et al.*, Improving Mixing Efficiency in Laminar-Flow Static Mixers with Baffle Inserts and Vortex Generators: A 3-D Numerical Investigation Using Corrugated Tubes, *Chemical Engineering and Processing-Process Intensification*, *193* (2023), 109530

[2] Bennour, E., *et al*., Numerical Investigation of Improved Mixing and Heat Transfer of a Shear-Thinning Fluid in Corrugated and Baffled Tube Systems, *Applied Thermal Engineering*, *268* (2025), 125863
[3] Kaid, N., *et al*., Investigating Hydrothermal Mass Transfer in an Extremely Low-Pressure Drop Passive Mixer: A 3-D Simulation Study, *Chemical Engineering Research and Design*, *200* (2023), Dec., pp. 1-11
[4] Menni, Y., *et al*., Numerical Analysis of Blade Height Ratio Effects on Mixing Efficiency and Energy Consumption in Triple-Blade Concentric Double-Helix Static Mixers, *Physics of Fluids*, *37* (2025), 2, 023602
[5] Meng, H., *et al.*, Experimental and Numerical Investigation of Turbulent Flow and Heat Transfer Characteristics in the Komax Static Mixer, *International Journal of Heat and Mass Transfer*, *194* (2022), 123006
[6] Meng, H., *et al*., A numerical study of mixing performance of high-viscosity fluid in novel static mixers with multitwisted leaves. Industrial & Engineering Chemistry Research, *53* (2014), 10, pp. 4084-4095
[7] Meng, H., *et al*., Chaotic Mixing Characteristics in Static Mixers with Different Axial Twisted-Tape Inserts, *The Canadian Journal of Chemical Engineering*, *93* (2015), 10, pp. 1849-1859
[8] Yu, Y., *et al.*, Investigation of Enhancing Heat Transfer in Three Kenics Static Mixer Utilizing Muti-Objective Optimization, *International Journal of Thermal Sciences*, *214* (2025), 109911
[9] Yu, Y., *et al*., Numerical Analysis of Thermal Dynamics and Mixing Performance in the Blade-Type Static Mixers, *Journal of Mechanical Science and Technology*, *36* (2022), 7, pp. 3701-3716
[10] Liao, W., Jing, D., Experimental Study on Fluid Mixing and Pressure Drop of Mini-Mixer with Flexible Vortex Generator, *International Communications in Heat and Mass Transfer*, *142* (2023), 106615
[11] Fan, S., *et al*., Emulsion polymerizations in a pilot-scale loop reactor with inline static mixers. Industrial & engineering chemistry research, *44* (2005), 15, pp. 5483-5490
[12] Kundra, M., *et al*., Continuous Flow Hydrogenation of Flavorings and Fragrances Using 3-D-Printed Catalytic Static Mixers, *Industrial & Engineering Chemistry Research*, *60* (2021), 5, pp. 1989-2002
[13] Albertazzi, J., *et al.*, Mixing Efficiency and Residence Time Distributions of a Side-Injection Tubular Reactor Equipped with Static Mixers, *Industrial & Engineering Chemistry Research*, *60* (2021), 29, pp. 10595-10602
[14] Coroneo, M., *et al*., Computational Fluid Dynamics Modelling of Corrugated Static Mixers for Turbulent Applications, *Industrial and Eng. Chemistry Research*, *51* (2012), 49, pp. 15986-15996
[15] Cheng, W., *et al*., Computational Fluid Dynamics Simulation of Mixing Characteristics and Light Regime in Tubular Photobioreactors with Novel Static Mixers, *Journal of Chemical Technology & Biotechnology*, *91* (2016), 2, pp. 327-335
[16] Chakleh, R., Azizi, F., Performance Comparison Between Novel and Commercial Static Mixers under Turbulent Conditions, *Chemical Engineering and Processing-Process Intensification*, *193* (2023), 109559
[17] Bennour, E., *et al*., Numerical investigation on a chaotic passive micromixer based on square chambers connected with different channel shapes for enhancing the mixing process. Industrial & Engineering Chemistry Research, *63* (2024), 6, pp. 2861-2874
[18] Faradonbeh, V. R., *et al*., Advancing Micromixing Techniques: The Role of Surface Acoustic Waves and Fluid-Structure Interaction in Non-Newtonian Fluids, Micro-Fluidics and Nanofluidics, *29* (2022), 3, 12
[19] Fallah, D. A., *et al*., Numerical Investigation of Heat Transfer and Mixing Process Phenomena Inside a Channel Containing a Triangular Bluff Body and Elastic Micro-Beam: Gap Spacing and Geometric Characteristic Effects, *Micro-fluidics and Nanofluidics*, *26* (2022), 3, 18
[20] Basu, S., Dirbude, S.B.. Flow, Thermal, and Mass Mixing Analysis in a T-Shaped Mixer, in: *Scientific and Technological Advances in Materials for Energy Storage and Conversion*, Eds. Sikarwar, B. S., Sharma, S. K., FLUTE 2023. Lecture Notes in Mechanical Engineering. Springer, Singapore, Singapore, 2024
[21] Wang, C., *et al*., Study on Mixing Performance of Perforation Static Mixers Applied to High Viscosity Polymer Mixing, *The Canadian Journal of Chemical Engineering*, *103* (2025), 6, pp. 2953-2964
[22] Stec, M., Synowiec, P. M., Study of Fluid Dynamic Conditions in the Selected Static Mixers Part I-Research of Pressure Drop, *The Canadian Journal of Chemical Engineering*, *95* (2017), 11, pp. 2156-2167
[23] Rauline, D., *et al*., Numerical Investigation of the Performance of Several Static Mixers, *The Canadian Journal of Chemical Engineering*, *76* (1998), 3, pp. 527-535
[24] Meng, H., *et al*., Heat Transfer Enhancement of Nanofluids in a Four-Blade LPD Static Mixer, *International Journal of Heat and Fluid-Flow*, *106* (2024), 109289
[25] Yu, Y., *et al*., A Comprehensive Review of Gas-Liquid Two-Phase Flow in Static Mixers, *Chemical Engineering and Processing-Process Intensification*, *216* (2025) 110434

Paper submitted: March 17, 2025
Paper revised: June 18, 2025
Paper accepted: July 29, 2025